Berk-Breizman and diocotron instability testcases

M. Mehrenberger, N. Crouseilles, V. Grandgirard, S. Hirstoaga, E. Madaule, J. Petri, E. Sonnendrücker

Université de Strasbourg, IRMA (France); INRIA Grand Est, CALVI project; ANR GYPSI

AMVV, East Lansing (Michigan), 13 November 2012
www.egr.msu.edu/amvv2012

Outline

- Berk-Breizman testcase
- Diocotron instability testcase

The equation

The **Berk Breizman** system is given by $f(t, x, v)$ and $E(t, x)$,
$(x, v) \in [0, L] \times \mathbb{R}_v$ satisfying

- **Vlasov** for the distribution function f

$$\partial_t f(t, x, v) + v \partial_x f(t, x, v) + E(t, x) \partial_v f(t, x, v) = \nu_{\mathbf{a}}(F_0(v) - f(t, x, v))$$

- **Maxwell** for the electric field E

$$\partial_t E(t, x) = -\int_{\mathbb{R}_v} v(f(t, x, v) - \bar{f}(t, v))dv - \gamma_{\mathbf{d}} E(t, x)$$

$$\bar{f}(t, v) = \frac{1}{L} \int_0^L f(t, x, v)dx$$

Reference and physical context

R. G. L. Vann, Characterization of a fully nonlinear Berk-Breizman phenomonology, PhD thesis, University of Warwick, 2002.

- Classical **Vlasov-Poisson** system for $\nu_{\mathbf{a}} = \gamma_{\mathbf{d}} = 0$
- distribution function : addition of **source** $Q(v)$ and **loss** (friction)

$$Q(v) - \nu_{\mathbf{a}} f, \ Q(v) = \nu_{\mathbf{a}} F_0(v)$$

- electric field : addition of **dissipative** term

$$-\gamma_{\mathbf{d}} E(t, x)$$

Bump on tail

Initial data :

$$f(0, x, v) = (1 + \alpha \cos(kx))F_0(v),$$

with equilibrium distribution function : **beam-bulk interaction**

$$F_0(v) = F_{\text{bulk}} + F_{\text{beam}},$$

$$F_{\text{bulk}} = \frac{\eta}{v_c \sqrt{2\pi}} \exp\left(-\frac{1}{2}\left(\frac{v}{v_c}\right)^2\right),$$

$$F_{\text{beam}} = \frac{1 - \eta}{v_t \sqrt{2\pi}} \exp\left(-\frac{1}{2}\left(\frac{v - v_b}{v_t}\right)^2\right),$$

Physical parameters :
$v_b = 4.5, v_c = 1, v_t = 0.5, \eta = 0.9, \alpha = 0.01, L = 4\pi, \ k = \frac{2\pi}{L}.$

Bump on tail : source and loss term

RHS of Vlasov rewrites

$$\nu_a F_{\text{beam}} - \nu_a(f - F_{\text{bulk}})$$

- first term : **injected beam**
- second term : similar to a **Krook collision operator**

Numerical difficulties

- use of Maxwell instead of Poisson
    - basic schemes can lead to **cumulative error in electric field**
    - simple framework for testing well-adapted solvers
    - validity of the schemes can be assessed by comparing with Poisson (case $\nu_a = \gamma_d = 0$)
- bump on tail distribution with several vortices ($k = 3\frac{2\pi}{L}$, $L = 20\pi$)
    - already difficult for Vlasov-Poisson ($\nu_a = \gamma_d = 0$)
    - empirical observation of the numerical schemes :
        - either **too diffusive** behaviour
        - either **bad transition**, when the vortices merge

Numerical procedure : a Vlasov-Ampere type scheme

Time splitting

$$(f^n, E^{n-1/2}) \rightarrow (f^{n+1}, E^{n+1/2})$$

- **1/2 advection in** x : solve $\partial_t f + v \partial_x f = 0$ during $\Delta t/2$.
- **1/2 collision** : solve $\partial_t f = \nu_a(f - F_0)$ during $\Delta t/2$.
- compute the new electric field $E^{n+1/2}$

$$\frac{E^{n+1/2} - E^{n-1/2}}{\Delta t} = -\mathbf{J^n} - \gamma_d \frac{E^{n+1/2} + E^{n-1/2}}{2}.$$

- **advection in** v : solve $\partial_t f + E^{n+1/2} \partial_v f = 0$ during Δt.
- **1/2 collision** : solve $\partial_t f = \nu_a(f - F_0)$ during $\Delta t/2$.
- **1/2 advection in** x : solve $\partial_t f + v \partial_x f = 0$ during $\Delta t/2$.

Reconstruction of the current J^n

- Basic reconstruction **J0=J_basic**
- Vanner (reformulated) reconstruction **J2=J_vanner**
- New reconstruction **J1=J_new**

The different schemes can be evaluated by comparing with
P=Poisson, in the case $\nu_a = \gamma_d = 0$.

The basic J^n reconstruction : **J0=J_basic**

We compute the current J^n directly from f^n, that is

$$J^n(x) = \int_{\mathbb{R}} v \left(f^n(x, v) - \bar{f}^n(v) \right) dv.$$

- like for Vlasov-Maxwell PIC simulations, this basic current computation can lead to bad results (the problem of **charge conservation**)
- a way of correction is to **define the current** in another way

The J^n reconstruction of Vanner : **J2=J_vanner**

- We compute J^{n-} from f after second $1/2$ collision of iteration $n-1$
- We compute J^{n+} from f after first $1/2$ collision of iteration n
- We define $J^n = \frac{J^{n-}+J^{n+}}{2}$.
- Remarks :
  - The original scheme of Vanner is here reformulated
  - This formulation permits to unify the different schemes (**J0,J1,J2**)

A new reconstruction **J1=J_new**

The charge density $\rho(t, x)$ is defined by $\rho(t, x) = \int_{\mathbb{R}} f(t, x, v) dv$.

- We compute $\rho^{n-1/2}$ after first 1/2 collision at iteration $n - 1$
- We compute $\rho^{n+1/2}$ after first 1/2 collision at iteration $n + 1$
- $\partial_x J^n$ is obtained from **charge conservation equation**

$$\frac{\rho^{n+1/2} - \rho^{n-1/2}}{\Delta t} + \partial_x J^n = \nu_a(1 - \frac{\rho^{n+1/2} + \rho^{n-1/2}}{2})$$

- J^n is obtained from $\partial_x J^n$ and $\int_0^L J^n(x) dx = 0$.

Numerical results

- Vlasov-Poisson : $\nu_a = \gamma_d = 0$

  - $N_x = N_v = 128$
  - $v_{\max} = 9$
  - $\alpha = 0.03$
  - $k = 0.3, L = \frac{2\pi}{k}$

- Periodic regime : $\nu_a = 0.03162, \ \gamma_d = 1$

  - $N_x = 64, \ N_v = 256$
  - $v_{\max} = 8$
  - $\alpha = 0.01$
  - $k = 0.3, L = \frac{2\pi}{k}$

  cubic splines for advection
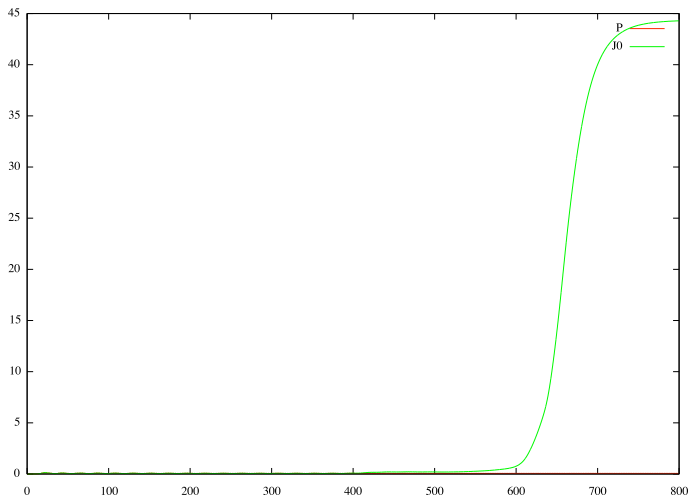 trapezoidal formula for Poisson

Vlasov-Poisson

FIGURE: $\frac{1}{L} \int E^2(t,x)dx$ vs time for **P** and **J0** for $\Delta t = 0.1$.

Vlasov-Poisson
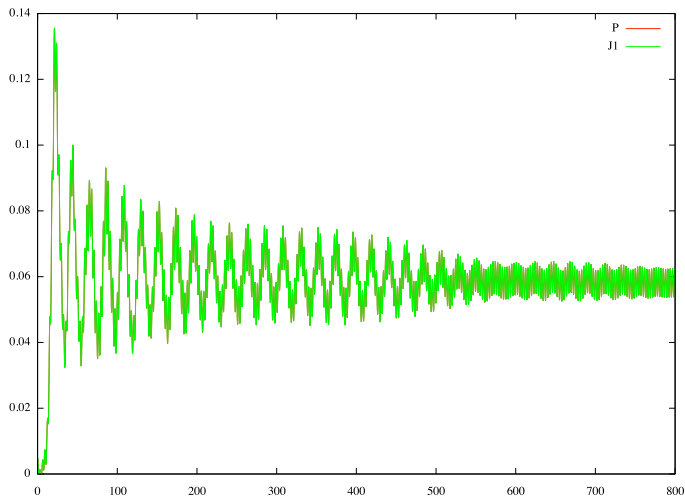
FIGURE: $\frac{1}{L}\int E^2(t, x)dx$ vs time for **P** and **J1** for $\Delta t = 0.1$.
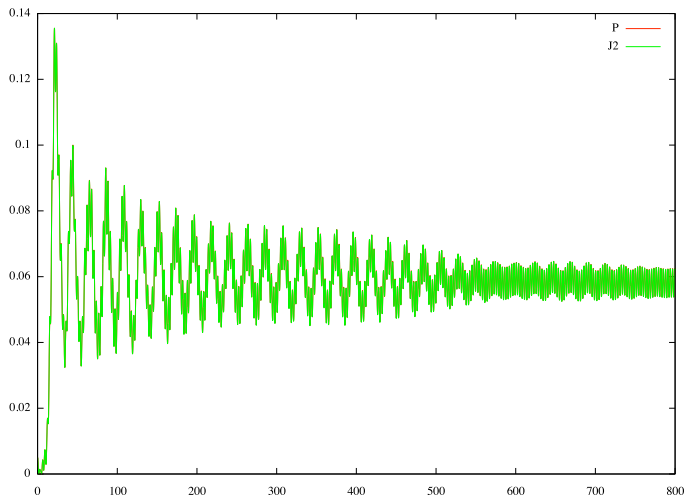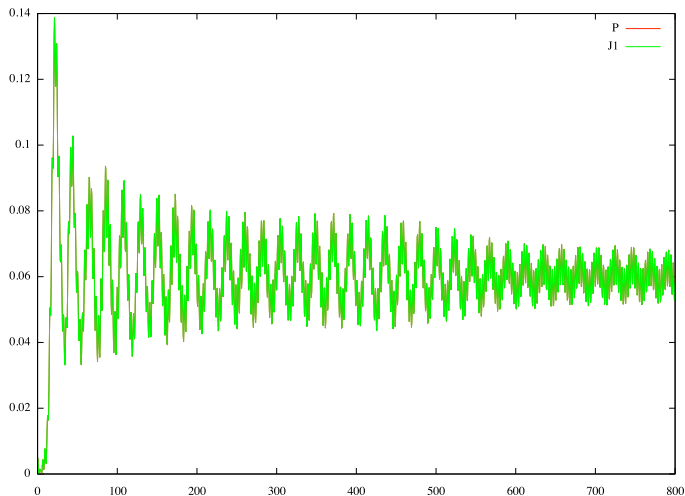
Vlasov-Poisson

FIGURE: $\frac{1}{L} \int E^2(t, x) dx$ vs time for **P** and **J2** for $\Delta t = 0.1$.

Vlasov-Poisson

FIGURE: $\frac{1}{L} \int E^2(t, x) dx$ vs time for **P** and **J1** for $\Delta t = 0.4$.
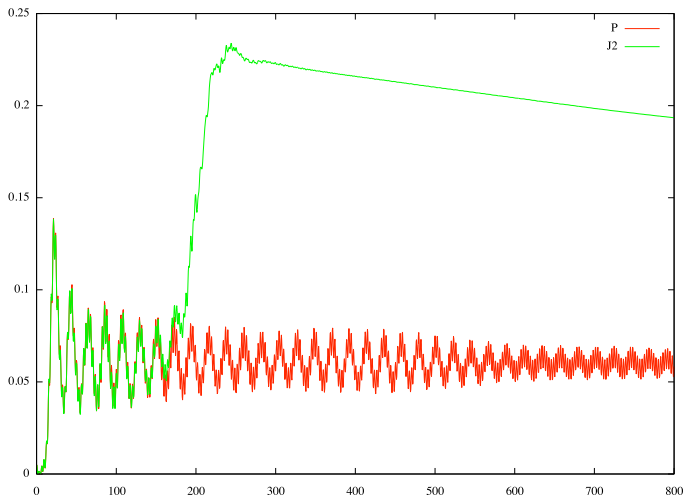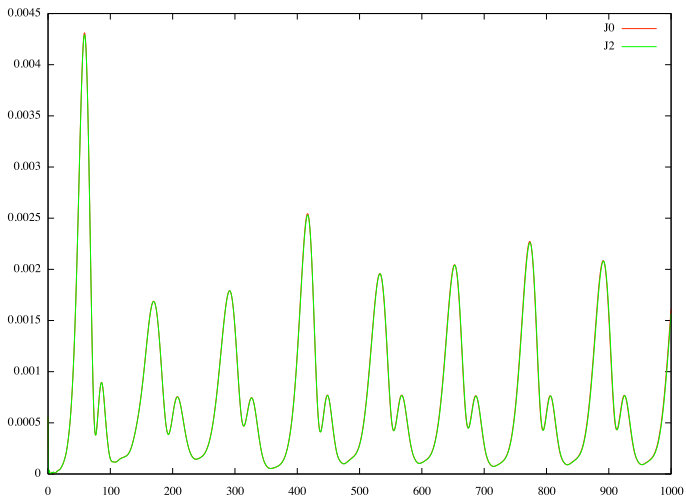
Vlasov-Poisson

FIGURE: $\frac{1}{L} \int E^2(t, x) dx$ vs time for **P** and **J2** for $\Delta t = 0.4$.

Periodic regime

FIGURE: $\frac{1}{L} \int E^2(t, x) dx$ vs time for **J0** and **J2** for $\Delta t = 0.1$

Periodic regime

FIGURE: $\frac{1}{L}\int E^2(t,x)dx$ vs time for **J1** and **J2** for $\Delta t = 0.1$
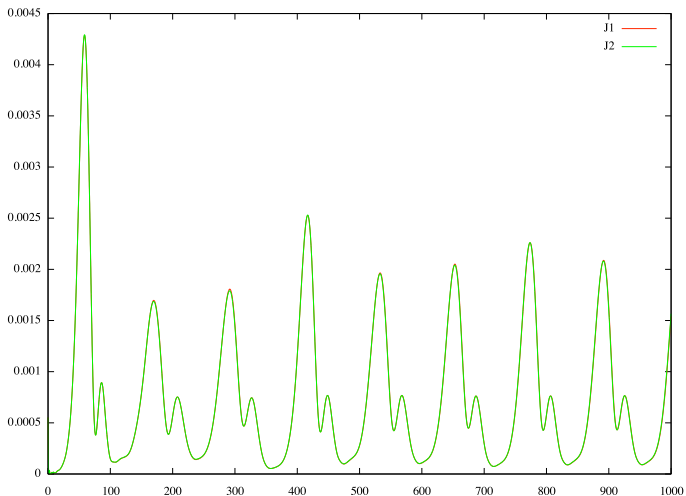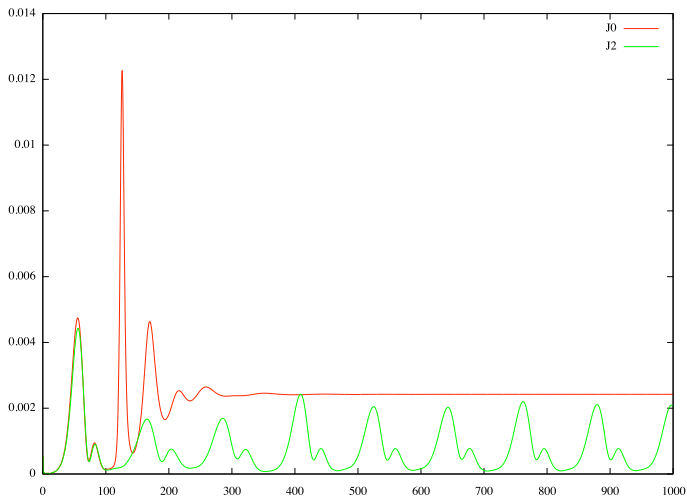
Periodic regime

FIGURE: $\frac{1}{L} \int E^2(t,x)dx$ vs time for **J0** and **J2** for $\Delta t = 0.4$.
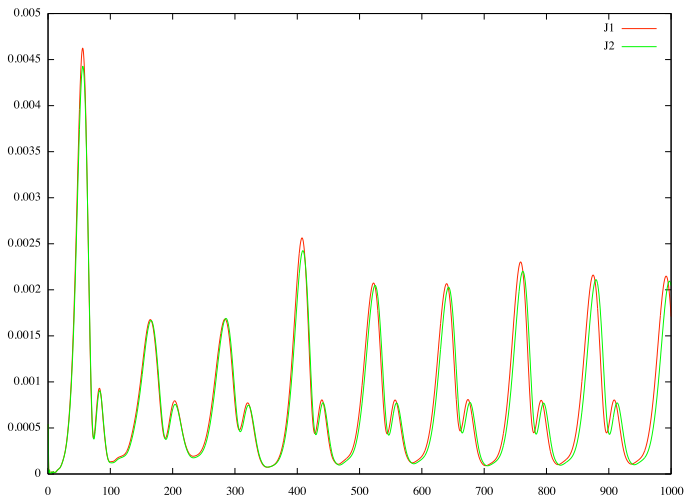
Periodic regime

FIGURE: $\frac{1}{L} \int E^2(t, x) dx$ vs time for **J1** and **J2** for $\Delta t = 0.4$.

LAG9 $N_x = N_v = 1024$ GPU double/simple precision
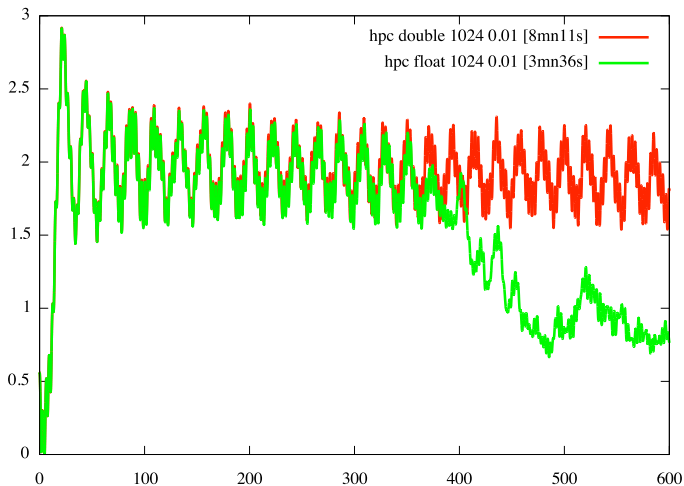

FIGURE: $\frac{1}{L} \int E^2(t, x) dx$ vs time for $\Delta t = 0.01$, $k = 3\frac{2\pi}{L}$, $L = 20\pi$

Conclusion/Perspectives

- Simple problem for charge conservation issue
- Simulation of different regimes
- Design of a new scheme adapted to this context
- Difficulties with several vortices
  - what can we hope numerically ?
- How to extend to higher dimension ?

Guiding center model in polar coordinates

The transport equation reads

$$\partial_t \rho - \frac{\partial_\theta \Phi}{r} \partial_r \rho + \frac{\partial_r \Phi}{r} \partial_\theta \rho = 0,$$

and is coupled with the Poisson equation for the potential $\Phi = \Phi(t, r, \theta)$

$$\partial_r^2 \Phi + \frac{1}{r} \partial_r \Phi + \frac{1}{r^2} \partial_\theta^2 \Phi = \rho.$$

Features

- center guide model generally studied in cartesian geometry
- same geometry as in toric gyrokinetic equations for tokamak modelling, for a poloidal section

  $\Rightarrow$ such intermediate testcase was missing, for testing numerical methods, which include geometrical effects (cf FSL)

- astrophysical testcase : diocotron instability (see Petri, Davidson)
- PIC method done by Petri
- references :
  - R. C. DAVIDSON, Physics of non neutral plasmas, 1990
  - J. PÉTRI, Non-linear evolution of the diocotron instability in a pulsar electrosphere : 2D PIC simulations, Astronomy & Astrophysics, May 7, 2009.

Work

- development of Vlasov semi-Lagrangian method for this testcase
- study of boundary conditions
  - conservation of electrostatic energy issue
  - linear stability issues

Electric energy

Proposition

We define the electric energy

$$\mathcal{E}(t) = \int_{r_{\min}}^{r_{\max}} \int_0^{2\pi} r|\partial_r \Phi|^2 + \frac{1}{r}|\partial_\theta \Phi|^2 dr d\theta.$$

We have

(i)

$$\mathcal{E}(t) = \int_0^{2\pi} [r\Phi\partial_r\Phi]_{r=r_{\min}}^{r=r_{\max}} d\theta - \int_{r_{\min}}^{r_{\max}} \int_0^{2\pi} \rho\Phi r dr d\theta.$$

(ii)

$$\partial_t\mathcal{E}(t) = 2\int_0^{2\pi} [r\Phi\partial_t\partial_r\Phi]_{r=r_{\min}}^{r=r_{\max}} d\theta - 2\int_0^{2\pi} [\Phi\rho\partial_\theta\Phi]_{r=r_{\min}}^{r=r_{\max}} d\theta.$$

BC1 boundary conditions

Proposition

We suppose Dirichlet boundary conditions at $r_{\min}$ and at $r_{\max}$:

$$\Phi(t, r_{\min}, \theta) = \Phi(t, r_{\max}, \theta) = 0.$$

Then the electric energy is constant in time :

$$\partial_t \mathcal{E}(t) = 0.$$

BC2 boundary conditions

Proposition

The electric energy is also constant in time if we suppose

(i) *Dirichlet boundary condition at $r_{\max}$: $\Phi(t, r_{\max}, \theta) = 0$*

(ii) *Inhomogeneous Neumann boundary condition at $r_{\min}$ for the Fourier mode 0 in θ :*

$$\int_0^{2\pi} \partial_r \Phi(t, r_{\min}, \theta) d\theta = Q,$$

where Q is a given constant.

(iii) *Dirichlet boundary condition at $r_{\min}$ for the other modes, which reads*

$$\Phi(t, r_{\min}, \theta) = \frac{1}{2\pi} \int_0^{2\pi} \Phi(t, r_{\min}, \theta') d\theta'$$

BC3 boundary conditions

Remark

We do not know whether the electric energy remains in constant in time when we consider the following boundary conditions :

  (i) Dirichlet at $r_{\max}$: $\Phi(t, r_{\max}, \theta) = 0$.

  (ii) Neumann at $r_{\min}$: $\Phi(t, r_{\min}, \theta) = 0$.

We consider the following initial data

$$\rho(0, r, \theta) = \begin{cases} 0, \ r_{\min} \leq r < r^-, \\ 1 + \varepsilon \cos(\ell\theta), \ r^- \leq r \leq r^+, \\ 0, \ r^+ < r \leq r_{\max}, \end{cases}$$

where ε is a small parameter.

The linear analysis is performed in Davidson, 1990

- **BC2** are considered
- Formulae for instability growth rate are explicit
- Formulae for **BC1** can be derived from **BC2** with good choice of Q
- Formulae can be adapted for **BC3**
- Values between **BC2** and **BC3** are very close
- numerical treatment of dispersion relation also studied with approximate growth rate

Numerical results

- Linear growth rate observed for corresponding Fourier mode
- Modes visible on distribution function plots, as in PIC simulation
- $\mathcal{E}_h(t) - \mathcal{E}_h(0)$ can increase or *decrease* with same growth rate
  - For PIC (Petri), $\mathcal{E}_h(t) - \mathcal{E}_h(0)$ increase with same growth rate
  - Continous model *conserves* the electric energy for **BC1** and **BC2**
- **BC2** and **BC3** simulations are near, particularly in the linear phase
- structures can merge in the non linear phase

Parameters

- $m = 7$
- $\varepsilon = 10^{-6}$
- $r_{\min} = 1$, $r_{\max} = 10$
- $r^- = 6$, $r^+ = 7$
- **BC2** boundary conditions
- classical semi-Lagrangian simulation
- $N_r = 512$, $N_\theta = 256$
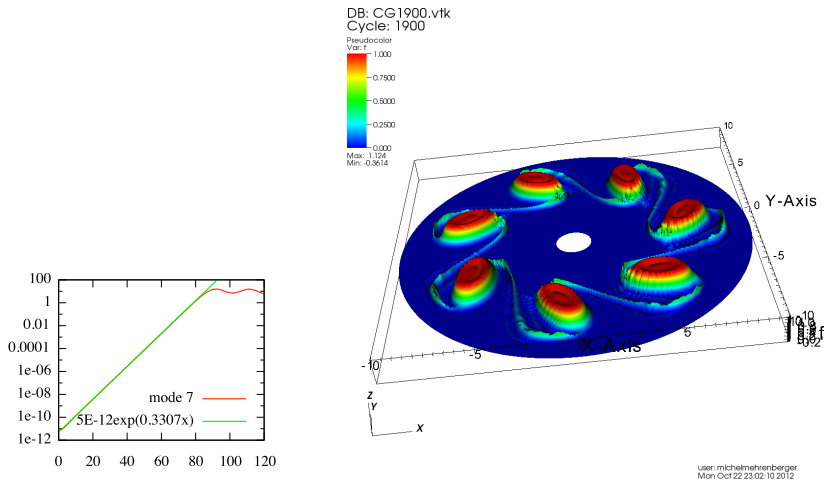- time step $\Delta t = 0.05$

FIGURE: Square modulus of the 7th Fourier mode of $\int_{r_{\min}}^{r_{\max}} \Phi(t, r, \theta)dr$ vs time t (left). Density ρ at $t = 95$ (right).

Conclusion/Perspectives

- validation of testcase for a grid based solver
- special boundary conditions treatment ; highlighting of **BC2**
- future use of this testcase, for testing numerical methods
    - 2D conservative remapping (P. Glanc)
    - curvilinear grids (A. Hamiaz)
    - gyroaverage operator (C. Steiner)